



Meso-mechanics simulation analysis of microwave-assisted mineral liberation

Qin Like, Dai Jun

*School of Architecture and Civil Engineering Xi'an University of Science and Technology, Xi'an 710054, P.R China
422576294@qq.com*

Yuan Liqun

School of Architecture and Civil Engineering, Liaocheng University, Liaocheng 252059, P.R China

ABSTRACT. Microwave-assisted crushing and grinding can improve efficiency and reduce energy consumption. This paper takes rock grains with galena and calcite as the research object to establish a two-dimensional computational model through the finite difference software FLAC2D. It analyzes the process and law of mineral boundary failure under microwave irradiation, and assesses the effects of four factors, namely, microwave irradiation time, power density, mineral crystal size, and mineral content, on mineral boundary failure. Results indicate an optimal microwave irradiation period for the rapid failure of mineral boundary. Moreover, irradiation time and energy consumption can be reduced by increasing the microwave power density. However, irradiation time and energy consumption are basically unchanged when the microwave power density is above a certain threshold. Mineral content slightly affects the microwave irradiation time, whereas mineral crystal size significantly affects the microwave irradiation time. In addition, a larger-sized mineral crystal requires less irradiation time and energy consumption to reach the same failure rate. However, irradiation time and energy consumption slightly change when the crystal size is larger than a certain value.

KEYWORDS. Microwave heating; Assisted liberation; Meso-mechanics simulation; Irradiation time; Energy consumption.

INTRODUCTION

Microwave is an ultra-high frequency electromagnetic wave with a wavelength of 1 mm~1 m. It can be used for heating [1]. Compared with conventional heating, microwave heating has advantages of internal heating, rapid heating, selective heating, and simple control; therefore, microwave heating is extensively used in various fields, such as food, agriculture, medical, and metallurgy [2-5]. Microwave heating can also be utilized for sorting minerals, which can effectively improve sorting efficiency and reduce energy consumption. Different minerals produce various heating characteristics under microwave irradiation due to diverse dielectric properties [6]. The results indicate that several gangue minerals, such as quartz, calcite, and muscovite, are classified as electromagnetic wave-transparent materials that are difficult to heat by microwave; however, some ores, primarily sulfide mineral, iron oxide ores, such as copper, lead sulfide, pyrite, manganese oxide, and many other useful minerals, are microwave-absorbing materials, which can be heated in a very short time in the microwave field [7, 8]. Therefore, in the microwave irradiation process, a large temperature

difference may form between the gangue and mineral, and a temperature stress may form, producing micro cracks on the mineral boundary and contributing to mineral liberation [9, 10].

Testing and numerical methods nowadays are chiefly adopted in microwave-assisted grinding and crushing studies. The test method is primarily used for determining the mineral temperature rising curve and the effect of auxiliary grinding. Some scholars have adopted the test method to examine the temperature rising characteristics of titanium concentrate and ilmenite in a microwave field using thermocouple [11, 12]. Xiaojuan Pan [13] investigated the temperature rising characteristics of manganese ore powder in a microwave field. Mamdouh Omranet et al. [14] placed the iron ore under microwave irradiation and scanned it via electron microscope (see Fig. 1). Their test results confirm that micro cracking occurs more easily between mineral and gangue through microwave heating than traditional heating. Shenghui Guo et al. [15] placed ilmenite under microwave irradiation and revealed that micro cracking occurs between useful mineral and gangue through microwave irradiation, which can effectively promote liberation between mineral and gangue.

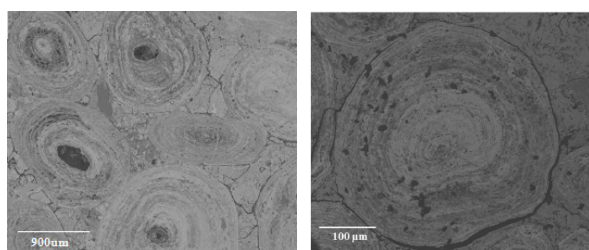


Figure 1: BSE image of micro crack distribution after microwave irradiation [14].

At present, measuring via tests the internal temperature and the stress and strain distribution of rocks under microwave irradiation is difficult. Qualitative analysis can be performed through scanning electron microscope for the generation and development of micro cracks in minerals under microwave irradiation. However, conducting quantitative research in this manner is difficult. Therefore, numerical methods have been primarily used for research in this field. Huijun Cui et al. [16] simulated the characteristic curve of the increasing temperature of carbon chrome ore powder in a microwave field using the finite element method. Some scholars have studied the internal temperature and the stress and strain distribution characteristics of a single crystal mineral through the finite difference method and finite element method, respectively [17-19]. A.Y. Ali et al. [20] confirmed the existence of micro cracks between mineral and gangue via the numerical method. Whittles et al. [21] analyzed the change of rock strength under microwave irradiation using the finite difference method. Although studies on microwave-assisted mineral liberation have achieved certain results, research on the characteristics and influencing factors of mineral liberation cracks remains scarce. Thus, this study takes rock grains with galena and calcite as the research object to investigate the distribution and evolution characteristics of mineral boundary failure under microwave irradiation using the finite difference method. It seeks to ascertain the mineral liberation mechanism under microwave irradiation, and to provide a theoretical basis for the selection of microwave source and optimized design of microwave equipment.

CALCULATION MODEL

Calculation Principal

The heat energy produced by microwave irradiation primarily depends on the microwave frequency and the electric field intensity. The quantity of heat produced by a material of unit volume can be calculated by the following formula:

$$P_d = 2\pi f \epsilon_0 \epsilon_r'' E_0^2 \tag{1}$$

where P_d denotes the power density of microwave (W/m^3), that is, the power of microwave transforming heat energy; f is the microwave divergence frequency (Hz); ϵ_r'' is the dielectric coefficient in a vacuum ($8.854 \times 10^{-12} F/m$); ϵ_0 is the medium dielectric loss factor; and E_0 is the effective value of the electric field (V/m). Given that the dielectric loss factor of calcite is 4×10^{-4} and that of galena is 13, under the irradiation by microwave, calcite absorbs little energy from the microwaves, and the non-production of heat by calcite in the calculation may be assumed [22].



The differential expression of the energy balance in FLAC has the form

$$-\nabla \cdot q^T + q_v^T = \frac{\partial \zeta T}{\partial t} \tag{2}$$

where q^T is the heat-flux vector in (W/m²), q_v^T is the volumetric heat-source intensity (W/m³) that is equated to the power density within the material, and ζT is the heat stored per unit volume (J/m³). In general, temperature changes may be spurred by changes in both energy storage and volumetric strain, and the thermal constitutive law relating those parameters may be expressed as

$$\frac{\partial t}{\partial t} = M_T \left(\frac{\partial \zeta T}{\partial t} - \beta_v \frac{\partial \epsilon}{\partial t} \right) \tag{3}$$

where M_T and β_v are material constants, and T is temperature.

FLAC considers a particular case of this law, for which $\beta_v = 0$ and $M_T = \frac{1}{\rho C_v}$. ρ is the mass density of the medium (kg/m³), and C_v is the specific heat at constant volume (J/kg°C).

The hypothesis is that strain changes negligibly affect the temperature. Such an assumption is valid for quasi-static mechanical problems involving solids. Accordingly, we may express

$$\frac{\partial \zeta T}{\partial t} = \rho C_v \frac{\partial T}{\partial t} \tag{4}$$

The substitution of Eq. (4) in Eq. (2) yields the following energy-balance equation:

$$-\nabla \cdot q^T + P_d = \rho C_v \frac{\partial T}{\partial t} \tag{5}$$

After the material is heated by microwaves, the strain resulting from temperature change can be expressed as

$$\epsilon_{i,j} = \alpha_{i,j} \Delta T_{i,j} \tag{6}$$

where $\epsilon_{i,j}$ denotes the strain; $\alpha_{i,j}$ is the thermal expansion coefficient (1/°C); and $\Delta T_{i,j}$ is the temperature change.

The stress produced by heat can be calculated by Hooke's law as follows.

$$\sigma_{i,j} = \frac{\epsilon_{i,j} E_{i,j}}{(1 - 2\nu_{i,j})} \tag{7}$$

where $\sigma_{i,j}$ denotes the thermal stress of unit i, j; $E_{i,j}$ is the elastic modulus of unit i,j (Pa); and $\nu_{i,j}$ is the Poisson's ratio of unit i, j.

Calculation Model

This paper takes the rock grains consisting of galena and calcite as the research object. The research object is simplified into a two-dimensional plane strain model, with a rock grain size of 10 mm × 10 mm, and square galena crystal's side length of 0.6 mm. For mesh generation in FLAC2D, the unit length is 0.05 mm; after generation, the model contains 40,000 units and 40,401 nodes. By writing a random distribution subroutine, in the case of a given mineral content, the galena crystal is randomly distributed within the calcite crystal, without human intervention in the distribution process. After the model is determined, a calcite unit near a galena crystal is defined as a mineral boundary element, as shown in Fig. 2. Mineral boundary occupies only one element, with a width of 0.05 mm.

Under microwave irradiation, the failure of mineral boundary elements is the root cause of the microwave-assisted mineral liberation. The calculation involves taking the mechanical state of the mineral boundary element as the monitoring object, and the ratio of the number of boundary elements around galena in the failure state to the total number of mineral boundary elements is defined as the mineral boundary element failure rate. During calculation and analysis, this study focused on mineral boundary element failure rate changes and the development law under different conditions of irradiation and mineral composition. Under microwave irradiation, the heated rock generates thermal strain and thermal stress. An element after yield is considered to be a failure element in this paper.

The calculation assumes several conditions. First, model boundaries are adiabatic, and no heat transfer occurs between the model and the surroundings. The initial temperature of the model is 25 °C. Only galena absorbs microwave energy under microwave irradiation. The model boundary is free of any constraint. Finally, contact between galena and calcite occurs in a fixed manner.

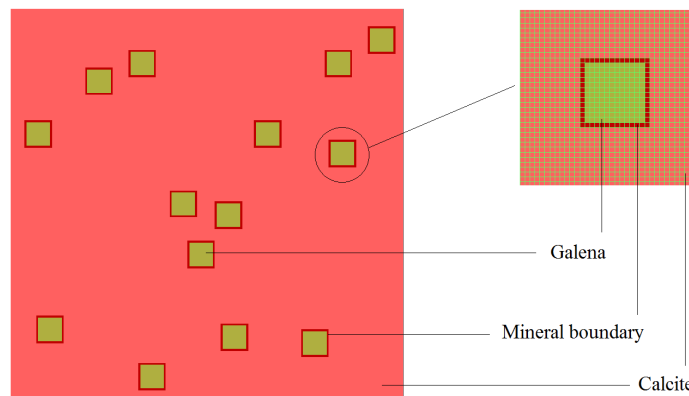


Figure 2: Geometric plot of computed model

Material parameters

The thermal conductivity and specific heat of galena and calcite are presented in Tab. 1, whereas the thermal expansion coefficient is shown in Tab. 2 [23, 24].

	Thermal conductivity coefficient (w/m °C)			Specific heat (J/kg °C)		
	25°C	100°C	227°C	25°C	227°C	727°C
Calcite	4.02	3.01	2.55	819	1051	1238
Galena	2.78	2.23	1.92	209	212	234

Table 1: Thermal conductivity and specific heat capacity of the mineral [23, 24].

	100°C	200°C	400°C	600°C
Calcite	1.31	1.58	2.01	2.4
Galena	6.12	6.1	6.32	6.68

Table 2: Thermal expansion coefficient of the mineral (10⁻⁵) [23, 24].

Both galena and calcite adopt the strain-softening model. This model is based on the Mohr–Coulomb model with non-associated shear and associated tension flow rules. Fig. 3 shows the one-dimensional strain softening model. The curve is linear to the point of yield; within this range, the strain is elastic only, $e = e^e$. After yield, the total strain is composed of elastic and plastic parts, $e = e^e + e^p$. The mechanical parameters are presented in Tab. 3 [21, 25].

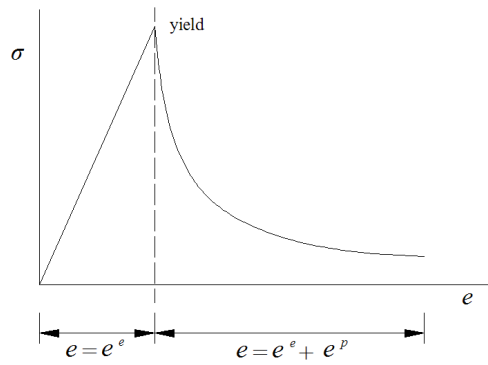


Figure 3: Stress-strain curve with strain-softening model.

	Density (kg/m ³)	Bulk modulus (GPa)	Shear modulus (GPa)	Peak strength (after 1% strain)			Residual strength(after 1% strain)		
				φ (°C)	c(MPa)	T(MPa)	φ_r (°C)	c_r (MPa)	T_r (MPa)
Calcite	2680	73.3	32.0	54	25	15	54	0.1	0
Galena	7597	58.6	31.9	54	25	15	54	0.1	0

Table 3: Mechanical parameters of the mineral [21, 25].

CALCULATION RESULTS AND ANALYSIS

The major factors that influence microwave-assisted mineral liberation include microwave power density, irradiation time, mineral content, and mineral crystal size. Mineral content pertains to the volume content, which is the ratio of the volume of mineral to that of total rock. To facilitate the comparison of the effects of different sizes of mineral crystals on mineral liberation, the size of crystals in the mineral herein is assumed to be similar.

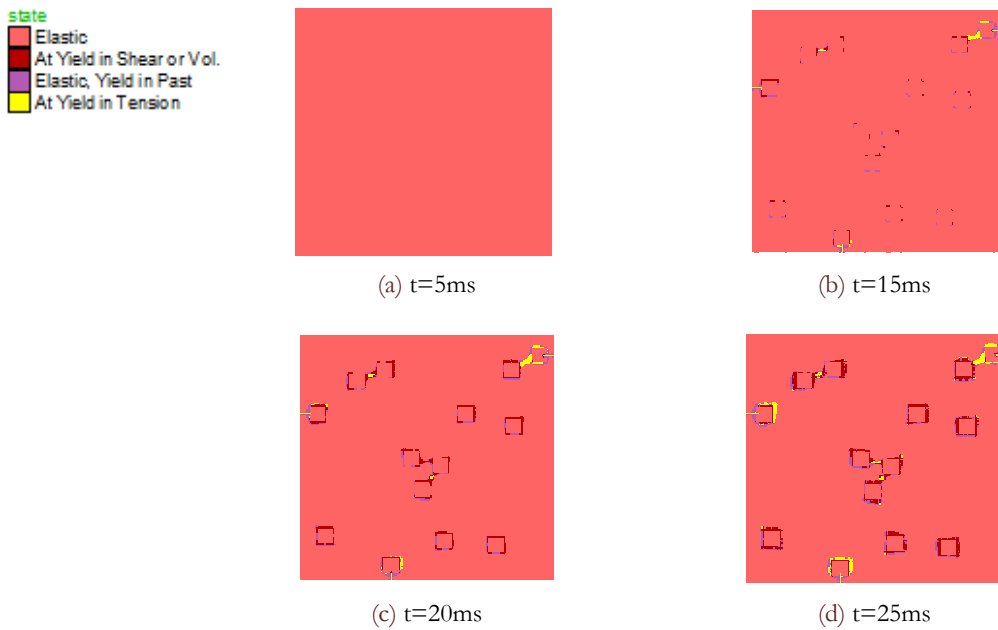


Figure 4: Distribution diagram of rock failure state ($P_d=10^9 W/m^3$).

Effect of irradiation time on mineral boundary failure

Fig. 4 shows the distribution of the mechanical state of rock at different irradiation times under the following conditions: mineral content of 5%, mineral crystal size of 0.6 mm, and microwave power density $P_d = 10^9 \text{ W/m}^3$. The figure demonstrates that as irradiation time increases, the rock changes from a completely elastic to a yield failure state. The boundary element around galena crystals near the rock border is destroyed first due to the free boundary of the mineral. Other boundary elements of galena crystals are gradually destroyed as irradiation time increases. Meanwhile, the failure elements among different crystals begin to link with each other. The development process of failure elements is similar to that obtained by Mamdouh Omran [14]. Fig. 4 also shows that the failure regions in the rock are concentrated at the boundary elements of galena crystals, which clearly signifies that microwave irradiation benefits mineral liberation. As indicated by the failure type, both shear and tensile failures occur. Tensile failure primarily occurs at the boundary regions of the sample and at the connecting regions of different mineral crystals. The rest of the failures are tensile.

Fig. 5 depicts the graph of mineral boundary failure rate over the irradiation time. The model consists of 728 mineral boundary elements. When irradiation time is 7.9 ms, some mineral boundary elements begin to step into a failure state. By contrast, when irradiation time is 12.5 ms to 20 ms, the mineral boundary failure rate rapidly increases from 11.67% to 91.07%, and mineral boundary element failure rate grows fastest during this irradiation period. When irradiation time is 28 ms, the boundary failure rate reaches 99.31%, after which time the rate does not increase further. This condition shows an optimal irradiation time for microwave-assisted mineral liberation. An irradiation time that is shorter than the optimal irradiation time averts the attainment of the mineral liberation effect. By contrast, an irradiation time that exceeds the optimal irradiation time wastes energy. Therefore, microwave-assisted mineral liberation and energy saving should critically determine the beginning and completion times of mineral boundary failure.

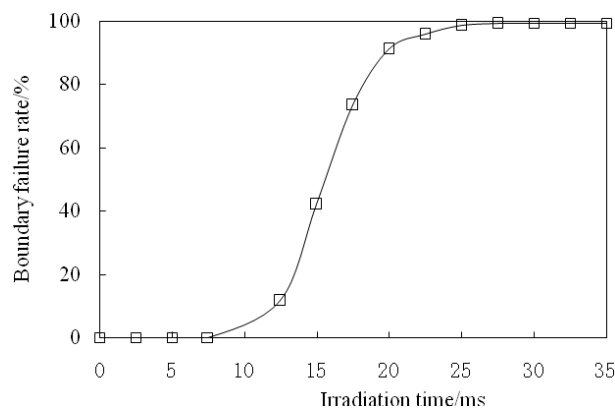


Figure 5: Relationship between failure rate around mineral boundary and irradiation time ($P_d=10^9 \text{ W/m}^3$).

Effect of microwave power density on failure rate

Fig. 6 illustrates the relationship between mineral failure rate and irradiation time at different microwave power densities under the condition in which mineral content is 5% and mineral crystal size is 0.6 mm. The figure demonstrates that as the power density increases during the optimal irradiation time, the growth of the slope is larger and the boundary element requires a shorter time to complete the failure. When the power density reaches $12 \times 10^9 \text{ W/m}^3$, mineral boundary element failure requires 3.5 ms from beginning to completion. Moreover, when the power density reaches $3 \times 10^9 \text{ W/m}^3$, the time required is 0.72 ms. Meanwhile, as the power density increases, the beginning and completion times of mineral boundary element failure occur earlier.

Fig. 7 illustrates the relationship between irradiation time and power density when the mineral boundary failure reaches 95%. As shown in the figure, as power density increases, irradiation time decreases. When the power density increases from $0.5 \times 10^9 \text{ W/m}^3$ to $3 \times 10^9 \text{ W/m}^3$, irradiation time decreases most obviously from 83 ms to 4.95 ms. Furthermore, when the power density is greater than $3 \times 10^9 \text{ W/m}^3$, irradiation time decreases within a very small range. Fig. 8 shows the relationship between energy consumption and power density when the boundary failure reaches 95%. When the power density increases from $0.5 \times 10^9 \text{ W/m}^3$ to $12 \times 10^9 \text{ W/m}^3$, energy consumption decreases rapidly. When the power density is greater than $3 \times 10^9 \text{ W/m}^3$, energy consumption decreases slightly, and when it is more than $12 \times 10^9 \text{ W/m}^3$, energy consumption increases slowly. In general, when the microwave power density is greater than $3 \times 10^9 \text{ W/m}^3$, irradiation time and energy consumption slightly change. This condition signifies that irradiation time and energy consumption cannot be



decreased effectively by blindly increasing microwave power density. When the power density exceeds a threshold value, the excessive power density will increase the equipment cost.

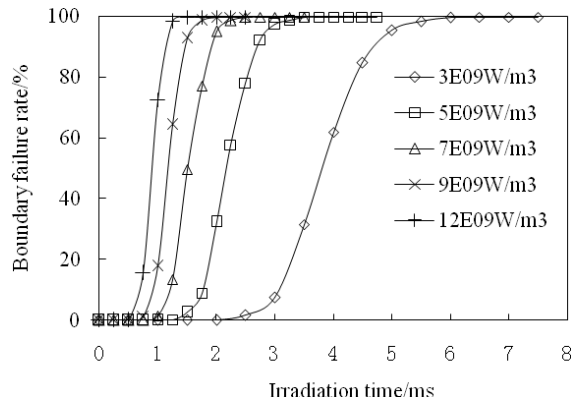


Fig. 6 Relationship between failure around mineral boundary and irradiation time.

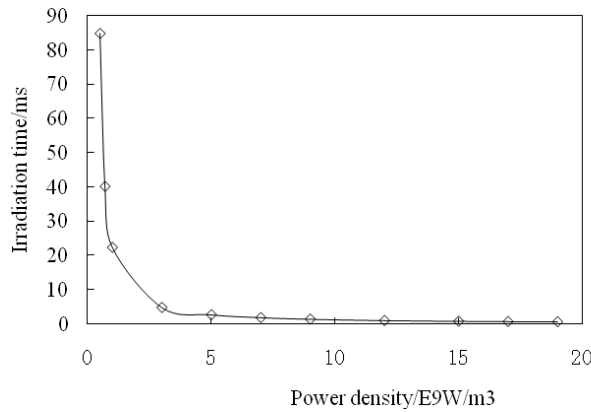


Fig. 7 Relationship between irradiation time and power density when the failure rate is 95%.

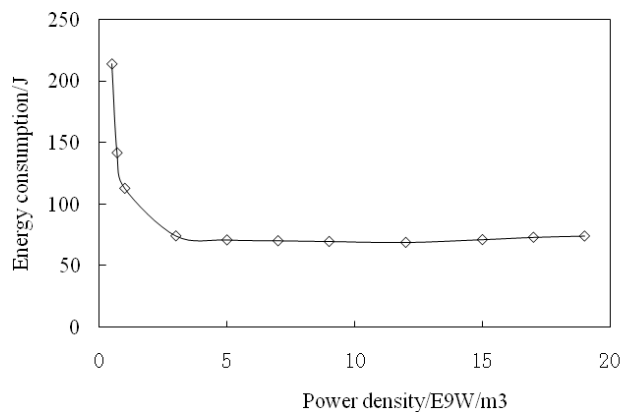


Fig. 8 Relationship between energy consumption and power density when the failure rate is 95%.

Effect of mineral content on rock failure state

Fig. 9 depicts the stress state for different mineral contents when the power density reaches $7 \times 10^9 \text{ W/m}^3$ and irradiation time is 20 ms. As shown in the figure, the mineral contents are different; however, at the same irradiation time, the

mineral boundary failure rates are all 94.5%. This outcome is principally attributed to the fact that the microwave heating is categorized as internal heating; under the same mineral crystal size, a similar mineral liberation effect is generated.

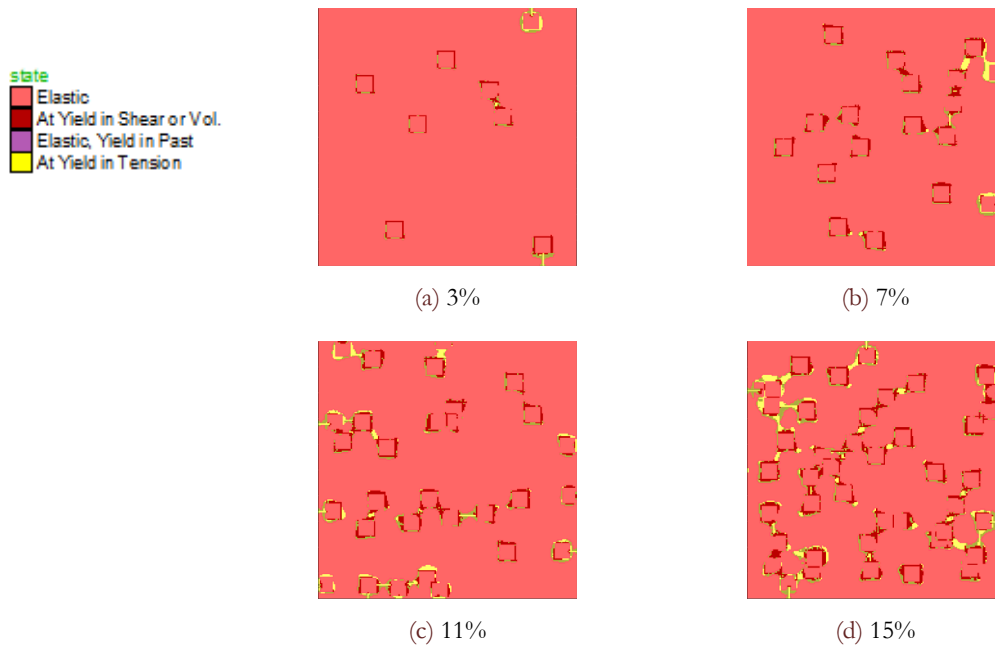


Figure 9: Distribution diagram of mechanical state of rock ($P_d=10^9 W/m^3$, $t=20$ ms).

Fig. 10 illustrates the relationship between mineral boundary failure rate and irradiation time with different mineral contents. Although mineral content curves are slightly different at the failure rate growth phase, the beginning and completion times are similar, that is, the same optimal microwave irradiation period, which indicates that the mineral content has a slight effect on the failure rate of the mineral boundary failure element.

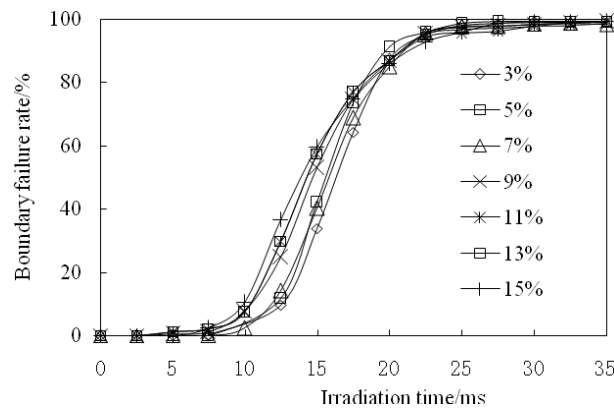


Figure 10: Relationship between failure around mineral boundary and irradiation time with different mineral content

Effect of mineral crystal size on rock failure state

Figs. 11 to 14 depict the relationship between mineral boundary failure rate curve and irradiation time, with a mineral content of 5%, microwave power density of $1 \times 10^9 W/m^3$, and galena crystal sizes of 0.2 mm, 0.4 mm, 0.8 mm, and 1.0 mm, respectively. As the mineral grains become larger, the slope of the growth curve is greater in the optimal microwave irradiation time; the smaller the mineral crystal is, the later the mineral boundary failure begins, and the later the failure completes. Moreover, as the mineral crystal is smaller, the irradiation time required by mineral boundary failure completion is longer.

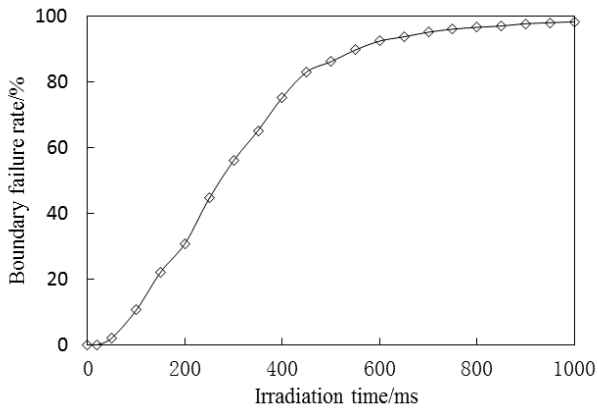


Figure 11: Relationship between failure around mineral boundary and irradiation time (0.2 mm).

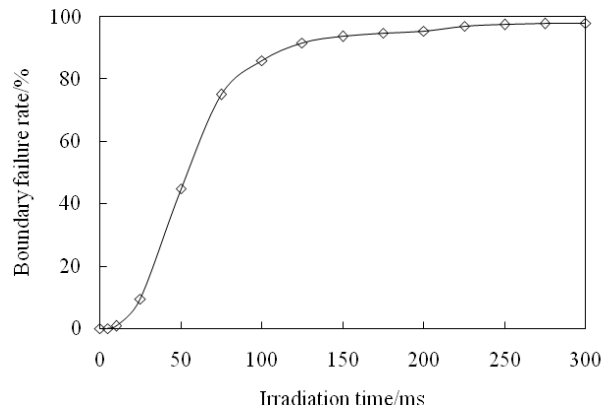


Figure 12: Relationship between failure around mineral boundary and irradiation time (0.4 mm).

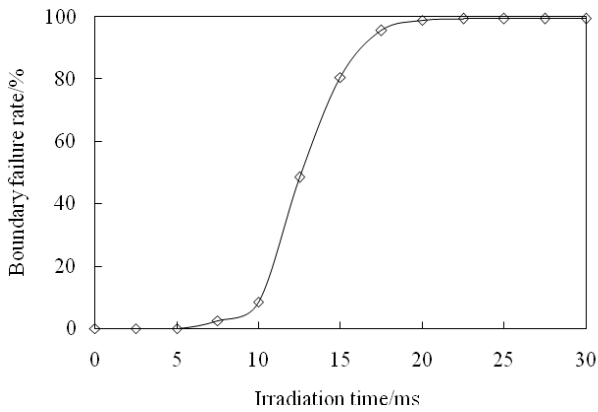


Figure 13: Relationship between failure around mineral boundary and irradiation time (0.8 mm).

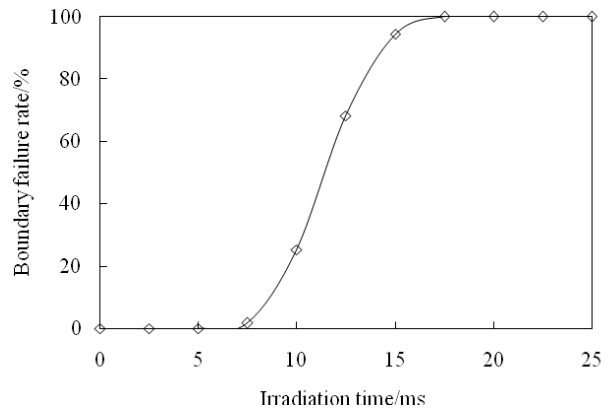


Figure 14: Relationship between failure around mineral boundary and irradiation time (1.0 mm).

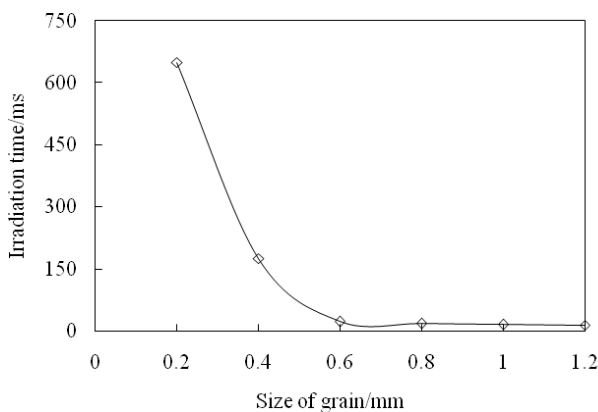


Figure 15: Relationship between irradiation time and grain size when the failure rate reaches 95%.

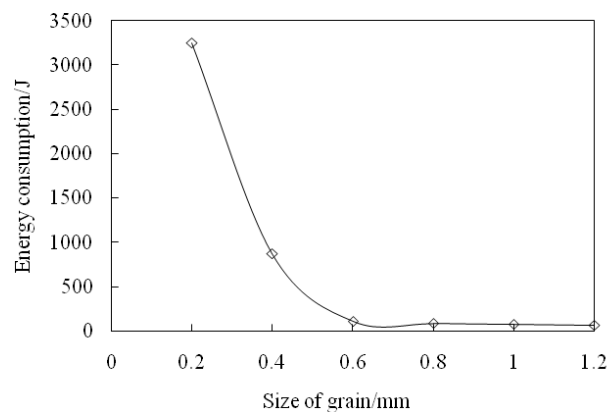


Figure 16: Relationship between energy consumption and grain size when the failure rate reaches 95%.

Fig. 15 illustrates the relationship between microwave irradiation time and grain size when the mineral failure rate reaches 95%. Fig. 16 shows the relationship between the corresponding energy consumption and grain size. As shown in the figures, as the mineral crystal becomes larger, irradiation time becomes shorter when the mineral boundary failure rate reaches 95%, and energy consumption is lower. When irradiation time decreases from 650 ms to 22 ms, energy consumption decreases from 3250 J to 85 J. Moreover, when the crystal size exceeds 0.6 mm, irradiation time and energy consumption substantially remain unchanged. The results of this method are consistent with those of other mineral



liberation methods, that is, the smaller the mineral crystal is, the harder the selection of mineral crystal becomes, and the more energy is consumed.

CONCLUSIONS

This study takes the mineral consisting of galena and calcite as the research object to establish a two-dimensional plane strain model and analyze the effects of microwave irradiation time, power density, mineral content, and mineral crystal size on microwave-assisted mineral liberation. It draws the following major conclusions:

- (1) Under the microwave irradiation, mineral boundary can be quickly destroyed in a specific period. An optimal irradiation period exists. When irradiation time is shorter than the beginning time of the optimal irradiation period, no failure occurs on the mineral boundary. By contrast, when irradiation time is longer than the end of the optimal irradiation period, more energy is wasted.
- (2) A greater microwave power density reduces the period for mineral boundary failure completion. The microwave irradiation time and energy consumption can be effectively reduced by improving the microwave power density. However, when the microwave power exceeds a certain value, the microwave irradiation period and energy consumption slightly change.
- (3) With the same microwave power density, when the mineral crystal size is constant, the mineral content has no effect on the optimal microwave irradiation time, and the beginning and completion times of failure exhibit no change. Moreover, mineral crystal size significantly affects the microwave irradiation time and energy consumption; the larger the mineral crystal, the shorter the irradiation time is, and the less energy consumption the mineral boundary failure requires. When the mineral crystal size exceeds a certain value, both irradiation time and energy consumption essentially remain unchanged.

ACKNOWLEDGEMENTS

This work was supported by the China Postdoctoral Science Foundation (2015M572580), the Foundation of Shaanxi Educational Committee (15JK1471), and the National Natural Science Foundation of China (No. 51174159).

REFERENCES

- [1] Jin, Q., *Microwave chemistry*. Science Press, Beijing, (1990) 214-216.
- [2] Duan, B., Zeng, L., Liu, P., Application and situation of microwave-assisted heating technology, *Ceramics*, 12(3) (2005)11-15.
- [3] Islam, M. M., Design of a microstrip antenna on duroid 5870 substrate material for ku and k-band applications. *Tehnicki Vjesnik*, 6(2) (2013) 71-77.
- [4] Lubikowski, K., Seebeck phenomenon, calculation method comparison, *Journal of Power Technologies*, 95(1) (2015) 63-67.
- [5] Czaplicka, K., Korol, K. B., et al., Model of eco-efficiency assessment of mining production processes, *Archives of Mining Sciences*, 1(2) (2015) 477-482.
- [6] Kingman, S. W., Vorster, W., Rowson, N. A., The influence of mineralogy on microwave assisted grinding, *Minerals engineering*, 22 (1) (2015) 160-163.
- [7] Zhong, L., Nano-structured Si/C/N composite powder produced by radio frequency induction plasma and its microwave absorbing properties, *Journal of Engineering Science and Technology Review*, 13(3) (2000) 313-327.
- [8] Liu, Q., Xiong, Y., Research on application mechanism of microwave in iron ores selective grinding, *Yunnan Metallurgy*, 6 (3) (1997) 25-28.
- [9] Kingman, S.W., Rowson, N.A., Microwave treatment of minerals- a review, *Minerals Engineering*, 11(11) (1998) 1081-1087
- [10] Kingman, S. W., Jackson, K., Recent developments in microwave assisted combination, *International Journal of Mineral Processing*, 74 (2004) 71-83



- [11] Huang, M., Peng, J., Lei, Y., Temperature rising behaviors and absorbing characteristics of titanium ore in microwave field, *Journal of Sichuan University: Engineering Science Edition*, 39 (2) (2007) 111-115.
- [12] Ouyang, H., Yang, Z., Xiong, X., et al., Research on the temperature rising curve and fluidizing leaching of ilmenite in microwave field, *Mining Metallurgical Engineering*, 30 (1) (2010) 73-75.
- [13] Pan, X., Chen, J., Zhao, M., Zhao, J., Research on temperature rising characteristics of carbon-bearing manganese carbonate powder after microwave heating, *New Technology & New Process*, 1 (2008) 55-58.
- [14] Omran, M., Fabritius, T., Mattila, R., Thermally assisted liberation of high phosphorus oolitic iron ore: A comparison between microwave and conventional furnaces, *Powder Technology*, 269 (2015) 7-14.
- [15] Guo, S., Chen, G., Microwave assisted grinding of ilmenite ore, *Transactions of Nonferrous Metals Society of China*, 21 (9) (2011) 2122-2126
- [16] Cui, H., Chen, J., Feng, X., Li, N., Numerical simulation for temperature rising curve of carbon-bearing chromium powder in microwave field, *China Metallurgy*, 17 (1) (2007) 30-35.
- [17] Jones, D.A., Kingman, S.W., Whittles, D.N., Understanding microwave assisted breakage, *Minerals Engineering*, 18 (2005) 659-669.
- [18] Wang, G., Radziszewski, P., Ouellet, J., Particle modeling simulation of thermal effects on ore breakage. *Computational Materials Science*, 43 (2008) 892-901.
- [19] Wang, Y., Djordjevic, N., Thermal stress FEM analysis of rock with microwave energy, *International Journal of Mineral Processing*, 130 (2014) 74-81.
- [20] Ali, A.Y., Bradshaw, S.M., Quantifying damage around grain boundaries in microwave treated ores, *Chemical Engineering and Processing*, 48 (2009) 1566-1573.
- [21] Whittles, D.N., Kingman, S.W., et al., Application of numerical modelling for prediction of the influence of power density on microwave-assisted breakage *International Journal of Mineral Processing*, 68 (2003) 71-91.
- [22] Chen, T.T., Dutrizac, J.E., Hague, K.E., et al., The relative transparency of minerals to microwave radiation, *Canadian Metallurgical Quarterly*, 23 (3) (1984) 349-354.
- [23] Touloukian, Y. S., Judd, W.R., *Physical properties of rocks and minerals*, McGraw-Hill Book Company, New York, (1981) 56-63.
- [24] Clark, S. P., *Handbook of physical constants*. Geological Society of America, New York, (1966) 415-436.
- [25] Bass, J.D., Elasticity of minerals, glasses, and melts. In: T.J. Ahrens, Editor, *Handbook of Physical Constants*, American Geophysical Union, Washington, DC, (1995) 45-63.